Biochemistry 1991, 30, 5157–5164

Correlations between Kinetic and X-ray Analyses of Engineered Enzymes: Crystal Structures of Mutants Cys → Gly-35 and Tyr → Phe-34 of Tyrosyl-tRNA Synthetase

Michael D. Fothergill and Alan R. Fersht*

MRC Unit for Protein Function and Design, University Chemical Laboratory, Lensfield Road, Cambridge CB2 1EW, U.K.

Received October 24, 1990; Revised Manuscript Received February 4, 1991

ABSTRACT: The crystal structures of two mutant tyrosyl-tRNA synthetases (TyrTS) are reported to test predictions from kinetic data about structural perturbations and also to aid in the interpretation of apparent strengths of hydrogen bonds measured by protein engineering. The enzyme–tyrosine and enzyme–tyrosyl adenylate complexes of the mutant, TyrTS(Cys → Gly-35), have been determined at 2.5- and 2.7-Å resolution, respectively. Residue Cys-35 is in the ribose binding site. Small rearrangements in structure are seen in the enzyme–tyrosine complex that are localized around the cavity created by the mutation. The side chain of Thr-51 moves to occupy the cavity, and Ile-52 adopts two significantly populated conformations, one as in the native enzyme and a second unique to the mutant. On binding tyrosyl adenylate, Ile-52 in the mutant crystal structure preferentially occupies the conformation observed in the native structure. The side chain at Thr-51 becomes disordered. The double-mutant test, which was designed to detect interactions between residues, had previously shown a discrepancy of some 0.4 kcal/mol on mutating Cys-35 and Thr-51 separately and together. A crystal structure of a second mutant, ΔTyrTS(Tyr → Phe-34), complexed with tyrosine has been determined at 2.7-Å resolution. Tyr-34 in wild-type enzyme makes a hydrogen bond with the phenolic oxygen of the bound tyrosine substrate. The mutant crystal structure was solved to discover whether or not a water molecule binds to the substrate instead of the hydroxyl of Tyr-34 as the interpretation of apparent binding energies from site-directed mutagenesis experiments hinges crucially on whether there is access of water to the mutated region.

Detailed analysis of any protein engineering experiment is aided by high-resolution structural information. Given the limitations of time and money, it is not practical to solve crystal structures of every mutant that is made, especially as many crystallographic studies have shown no structural changes on making conservative mutations. We have been developing methods of kinetic analysis that suggest when structural changes might be occurring. One example is the "double-mutant test" (Carter et al., 1984) in which residues are mutated singly and pairwise to see if individual effects of mutations are independent. The mutant TyrTS(Cys → Gly-35)[1] is one example where some double-mutant tests show nonadditivity. Further, in the preceding paper (Wells et al., 1991), there are unusually large changes in enthalpy and entropy of activation on that mutation.

Residue Cys-35 has the distinction of being the first residue in an enzyme of known three-dimensional structure to be modified by site-directed mutagenesis (Winter et al., 1982; Wilkinson et al., 1983). Initial crystallographic studies suggested that residue 35 hydrogen bonds to the 3′-OH of the ribose ring of tyrosyl adenylate in the activation reaction. The most recent refinements suggest that the S····O distance is too long for a good hydrogen bond but that the –SH binds to a water molecule (water-326) that makes a hydrogen bond with the 3′-OH (Brick et al. 1988). As Cys-35 is conserved in another aminoacyl-tRNA synthetase (Baker & Winter, 1982), mutations of the cysteine residue were constructed originally made to search for a contribution of the thiol group to catalysis (Winter et al., 1982). Construction of the free energy profile for the reaction

$$\mathrm{E + Tyr = E{\cdot}Tyr + ATP = E{\cdot}Tyr{\cdot}ATP = E{\cdot}Tyr\text{-}AMP{\cdot}PP_i = E{\cdot}Tyr\text{-}AMP + PP_i}$$

showed that Cys-35 contributes no binding energy to ATP in the E·Tyr·ATP complex but stabilizes the transition state for the formation of E·Tyr-AMP by 1.2 kcal/mol and Tyr-AMP by 1.6 kcal/mol, relative to a glycine at position 35 (Wells & Fersht, 1986). These values are at the upper end of the range 0.8–1.5 kcal/mol that is found experimentally for a large number of apparent H-bond energies determined in this laboratory and elsewhere (Fersht, 1988). The double-mutant test indicated an interaction between positions 35 and 51 (Carter et al., 1984). The sum of the individual changes in binding energy on mutating Cys → Gly-35 and Thr → Pro-51 differ by 0.4 kcal/mol from the total change in the double mutant Cys → Gly-35; Thr → Pro-51. The significance of the small nonadditivity is unknown. Could it be caused by the greater conformational flexibility of glycine, an observable movement in the protein or a change in solvation, or a series of effects so small as to be individually unobservable? Because of both the historical importance of this mutant and these questions, we report the crystal structures of TyrTS(Cys → Gly-35) complexed with tyrosine and tyrosyl adenylate, respectively.

Another outstanding question is whether or not water has access to a cavity created in a mutagenesis experiment. This is critical in the interpretation of measurements of binding energies from protein engineering experiments (Fersht, 1987b). Suppose, for example, one deletes a side chain that is a hydrogen-bond donor from an enzyme to a substrate. The mutant enzyme–substrate complex could then either have an unpaired hydrogen-bond acceptor on the substrate or water could act as the hydrogen-bond donor. A rigorous analysis shows that the change in binding energy on mutation, ΔG_{app}, is not equal to the incremental binding energy of the hydrogen bond (ΔG_{bind}) when the acceptor is left unpaired but ΔG_{app}

---

[1] Abbreviations: TyrTS, tyrosyl-tRNA synthetase; ΔTyrTS, TyrTS minus the C-terminal residues 316–417. ΔG_{app}, the apparent binding energy (Wells & Fersht, 1986), is the observed change in enzyme–ligand binding energy on making a mutation.

0006-2960/91/0430-5157$02.50/0

may equal ΔG_{bind} if water has ready access to the acceptor (Fersht, 1987a, 1988). To investigate this, we also report the crystal structure of TyrTS(Tyr → Phe-34). Crystallographic studies suggest that Tyr-34 hydrogen bonds to the hydroxyl oxygen of the tyrosine substrate (Brick & Blow, 1987). Construction of the free energy profile for eq 1 showed that Tyr-34 contributes 0.5 kcal/mol to the apparent binding energy in the E·Tyr complex (Wells & Fersht, 1986). The mutation should be a nondisruptive deletion; an –OH on a large side chain is replaced by an –H. The mutant appears to be well-behaved since, as shown in the preceding paper (Wells et al., 1991), there are just small changes in enthalpy and entropy of activation. TyrTS(Tyr → Phe-34) is a good candidate for studying the E·Tyr complex. Unlike other mutations in the tyrosine pocket, which drastically weaken substrate binding (Lowe et al., 1987), there is still tight binding of substrate (K_s for tyrosine is raised from 12 to 29 μM). We have chosen to use crystals of the truncated enzyme (ΔTyrTS) since the occupancy of tyrosine in the binding site is significantly better than that of the full-length molecule (Brick & Blow, 1987). [(Deletion of the C terminus of TyrTS abolishes the binding of tRNA but does not affect the formation of tyrosyl adenylate (Waye et al., 1983).]

EXPERIMENTAL PROCEDURES

Purification and Crystallization. TyrTS(Cys → Gly-35) was purified as described previously (Lowe et al., 1985). About 10 mg of the resulting pure protein was concentrated by ultrafiltration in Centricon 30 vessels (Amicon) to >10 mg/mL and crystallized by vapor diffusion (McPherson et al., 1982) in the presence of 1 mM tyrosine, which promotes the hexagonal plate form used for X-ray analysis. Crystals of the same form as those of wild-type enzyme (Irwin et al., 1976) were grown in 50% ammonium sulfate. A single large crystal (0.4 × 1.2 × 1.2 mm) was chosen for data collection. Crystals of the tyrosyl adenylate complex were grown by cocrystallization in the presence of saturating tyrosine, 10 mM ATP, 10 mM $MgCl_2$, and 100 mM Tris–acetate, pH 7.3, at 4 °C. ΔTyrTS(Tyr → Phe-34) was purified and crystallized as described above, except that poly(ethylene glycol) was the precipitant. Crystals were grown in the presence of 1 mM tyrosine, 10 mM $MgCl_2$, 100 mM Tris–acetate, pH 7.3, and 12% PEG. Crystals obtained were typically 0.4 × 0.8 × 0.8 mm and grew in the same form as the wild-type truncated enzyme (Brick & Blow, 1987). Two crystals were chosen for data collection.

Data Collection and Structure Refinement

TyrTS(Cys → Gly-35) Mutant. A complete set of data for the complex with tyrosine was collected to 2.5-Å resolution at the SRS facility in Daresbury (U.K.) by the oscillation method (Nyborg & Wonnacott, 1977) on flat films, in 40 min (2.0 GeV, ~250 mA). A total of 20 549 independent reflections (98.6% of the unique data) were measured out of a total of 43 782 giving an *R* merge of ~5.3%. No significant decay in the quality of diffraction was observed during the 30° rotation. A data set of poorer quality was collected for the cocrystal with tyrosyl adenylate. In this experiment, 19 912 independents (95.6% of the unique data) were measured out of a total of 42 188 reflections with an overall *R* merge of 10.6%. These data were good to 2.7-Å resolution. Cell dimensions: wild-type, $a = b = 64.5$ Å, $c = 238.1$ Å, $\alpha = 90°$, $\beta = 90°$, $\gamma = 120°$, space group $P3_121$; mutant plus tyrosine, $a = b = 64.6$ Å, $c = 238.1$ Å; mutant plus tyrosyl adenylate, $a = b = 64.4$ Å, $c = 238.6$ Å.

Difference Maps: Complex with Tyrosine. The first maps ($F_{\text{mut}}-F_{\text{wt}}$ and $3F_{\text{mut}}-2F_{\text{wt}}$) used phases calculated from the native structure. Subsequent maps (F_o-F_c and $3F_o-2F_c$) were computed before and after refinement, starting with wild-type coordinates (minus Cys-35 side-chain atoms) and then refitting the protein model where necessary by use of FRODO (Jones, 1985) supported on an Evans and Sutherland PS330 graphics system. The current residual after several cycles of restrained least-squares refinement by use of PROLSQ (Hendrickson, 1985) is 23.6% at 2.5-Å resolution compared with 21% (2.1-Å resolution) for the native structure (Blow et al., 1985).

Complex with Tyrosyl Adenylate. These were identical with the above except that tyrosyl adenylate was refined as the substrate and the resolution was 2.7 Å. The *R* factor did not differ significantly from that of the tyrosine complex. Refining alternate conformations of side chains at positions 35 and 51 in either the tyrosine or tyrosyl adenylate complex did not result in a significantly different *R* factor.

ΔTyrTS(Tyr → Phe-34) Mutant. A complete set of data for the complex with tyrosine was collected to 2.7-Å resolution at the SRS facility in Daresbury (2.0 GeV, ~250 mA, 0.88 Å). A total of 52 718 were reduced to 19 113 independent reflections (88.8% of the unique data) with an *R* merge of 8.4%. Cell dimensions: truncated wild-type plus tyrosine, $a = 95.5$ Å, $b = 67.1$ Å, $c = 61.4$ Å, $\alpha = 90°$, $\beta = 90.78°$, $\gamma = 90°$, space group $P2_1$; mutant plus tyrosine $a = 95.3$ Å, $b = 67.3$ Å, $c = 61.3$ Å, $\alpha = 90°$, $\beta = 90.82°$, $\gamma = 90°$.

Difference Maps: Complex with Tyrosine. Electron density maps were computed and displayed as described above, with the use of phases calculated from the native structure of the truncated enzyme (Brick & Blow, 1987). The current residual after several cycles of restrained least-squares refinement is 17.9% at 2.7-Å resolution (rms deviation in bond lengths is 0.018 Å compared with 18.7% (2.5-Å resolution, rms deviation 0.017 Å) for the native structure (Brick & Blow, 1987).

RESULTS

TyrTS(Cys → Gly-35) Mutant

Complex with Tyrosine. The initial map ($F_{\text{mut}}-F_{\text{wt}}$; wild-type phases) at 2.5-Å resolution contained a large negative peak (Figure 1) corresponding to the wild-type sulfur atom (and β carbon) of Cys-35. The F_o-F_c map shows two peaks adjacent to Thr-51 and Ile-52 (Figure 2). Inspection of the $3F_o-2F_c$ map showed the density of the side chain at Ile-52 to be contiguous with the new density, and this was interpreted as an alternate side-chain conformation (Figures 2 and 3). The conventional interpretation of this is that the side chain exists in two conformational states, each of which is significantly occupied and ordered. In this case, one state adopts the wild-type conformation and the other differs. The other peak was the β carbon of Thr-51, and the side chain had to be modeled into the $3F_o-2F_c$ map in a new conformation (Figures 2 and 3). The Thr-51 exists in one conformation only. Both the mutant and native torsion angles (Figure 3) are found with similar incidence in existing tertiary structures (Ponder & Richards, 1987). The main chain conformation was almost unchanged (rms deviation from native, 0.10 Å) and the structure is effectively isomorphous (overall rms deviation, 0.22 Å).

Complex with Tyrosyl Adenylate. This was treated in exactly the same way, with use of the models from the tyrosine structure. The electron density for the adenylate is shown in Figure 4. In order to compare the electron density for the Thr-51 and Ile-52 side chains in the tyrosine and tyrosyl adenylate structures, F_o-F_c and $3F_o-2F_c$ maps were computed with models without these side chains. It is not possible to refine the occupancies of these side-chain conformations at the resoltuion of the data. In practice, both data sets were refined separately in each alternate side-chain conformation.

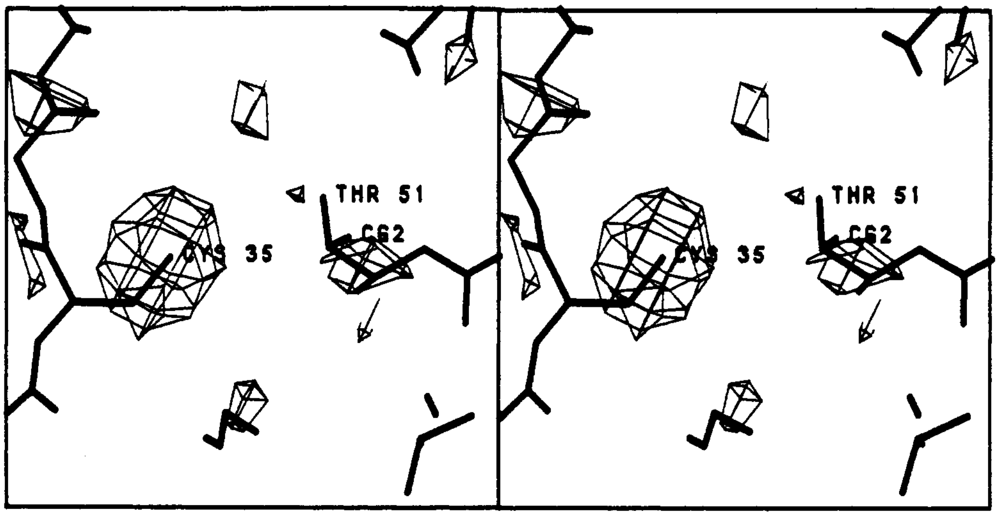

FIGURE 1: Difference electron density map of the Cys → Gly-35 mutant enzyme complexed with tyrosine ($F_{mut}-F_{wt}$, α_{wt}) at 2.5-Å resolution. Contouring is at 3σ, negative electron density shown only. The peak over the side chain of residue 35 suggests that the cysteinyl group is not present in the mutant structure.

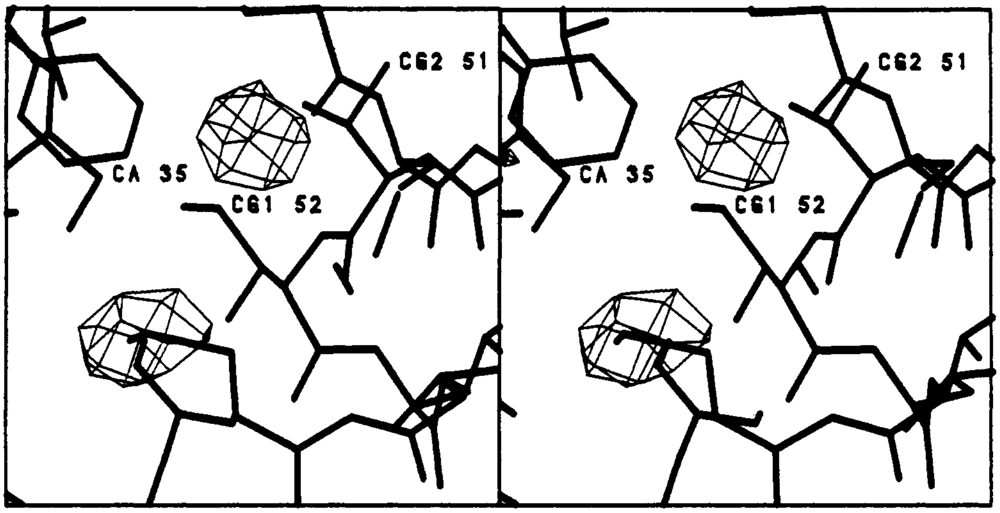

FIGURE 2: Difference electron density map of the Cys → Gly-35 mutant complexed with tyrosine (F_o-F_c, α_{calc}) after five cycles of refinement. Contouring is at 3σ, positive density shown only. The two peaks adjacent to Thr-51 and Ile-52 suggest that these residues have new, different conformations relative to the wild-type structure.

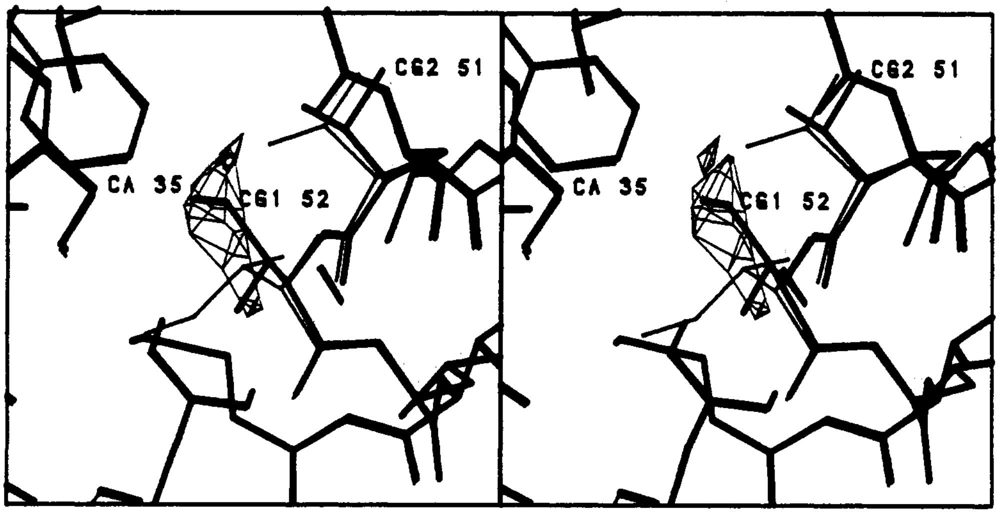

FIGURE 3: Difference electron density map of the Cys → Gly-35 mutant enzyme–tyrosine complex (F_o-F_c, α_{calc}) after refitting the model with the new conformations (shown in thin line) for Thr-51 and Ile-52 and refining them. Contouring is at 3σ, positive density shown only. The peak adjacent to Ile-52 shows that the native conformation (shown in heavy line) is still partly occupied in the mutant structure. After 10 cycles of refinement, the model differed as follows: Thr-51 $\chi 1$ native 62°, mutant −65°; Ile-52 $\chi 1$ native −64°, mutant −166°; $\chi 2$ native −161°, mutant 56°.

The models resulting from this process were almost identical (main chain rms deviation, 0.11 Å; overall, 0.19 Å) and were used to compute the omit maps. Inspection of the difference density (Figures 5 and 6) clearly shows that when tyrosyl adenylate is present, the alternate conformation at Ile-52 appears to have almost reverted to the wild type and the density

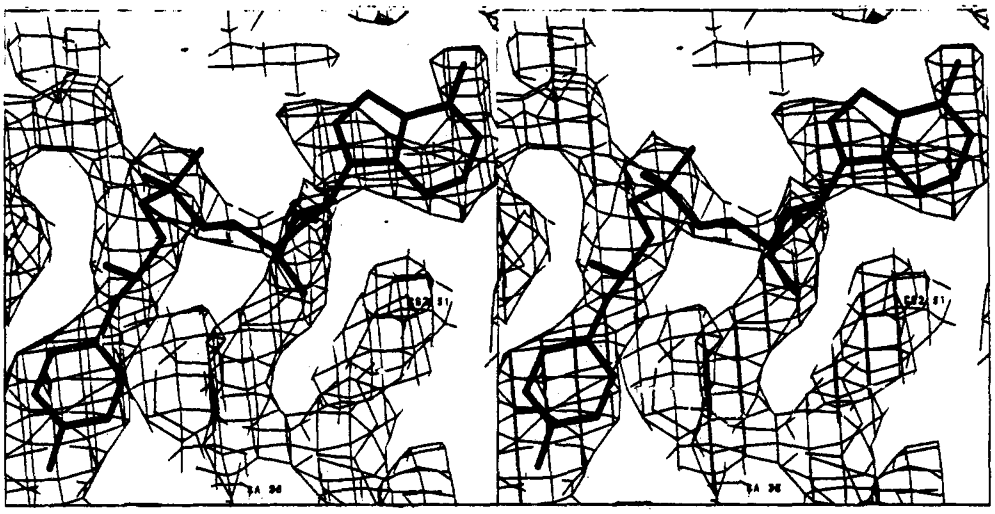

FIGURE 4: A second set of crystallographic data was collected for the Cys → Gly-35 mutant in the presence of tyrosine and MgATP. The 2.7-Å ($3F_o$–$2F_c$, α_{calc}) electron density map calculated with tyrosyl adenylate omitted from the model shows that there is significant occupancy of tyrosyl adenylate in this structure. Contouring is at 1σ.

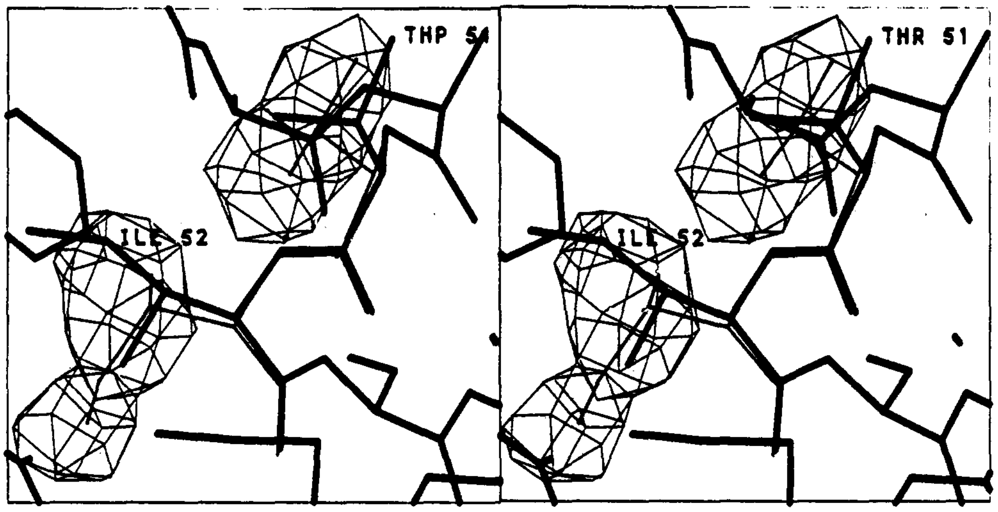

FIGURE 5: Difference electron density map (F_o–F_c, α_{calc}) at 2.5-Å resolution of the Cys → Gly-35 mutant complexed with tyrosine, where Thr-51 and Ile-52 side chains have been removed from the model. Contouring is at 3σ, positive density shown only. The two peaks give an unbiased representation of the conformation of Thr-51, and in particular, the relative occupancies of the two conformations (native and mutant in heavy and thin line, respectively) of that of Ile-52.

for Thr-51, although less easy to interpret, is of a different shape. In an effort to model these changes, the coordinates of the conformations of both Thr-51 and Ile-52 (wild type and mutant in each case) have been used to calculate, and hence model, density for these side chains. By varying the occupancies of the different conformations, it is possible to produce reasonably convincing representations of the observed density.

ΔTyrTS(Tyr → Phe-34) Mutant

Complex with Tyrosine. The initial map (F_{mut}–F_{wt}; wild-type phases) at 2.7-Å resolution showed a negative peak (Figure 8) corresponding to the hydroxyl oxygen of Tyr-34. Inspection of the $3F_o$–$2F_c$ map calculated after refining the mutant model shows convincing density for the substrate and Phe-34 (Figure 9). The occupancy of the substrate must be close to full, since the temperature factors after refinement are low; the mean B value for the tyrosine bound in the A subunit was 7.12 Å^2 compared with 10.5 Å^2 in the native structure; that of the B subunit was 5.9 Å^2 relative to the native 7.51 Å^2. In addition, the temperature factor for the side chains of residue 34 fell from 7.00 and 11.45 Å^2 in the native structure to 4.63 and 6.78 Å^2 in the mutant A and B subunits, respectively. No other features are present and there is no room for a water to bind in the pocket created in this mutation (Figure 10).

DISCUSSION

The quality of the X-ray data from these mutants and the disordered C-terminal region of the full-length tyrosyl-tRNA synthetase limits the interpretation of the results. It is possible to detect, for example, that there is a new conformation of the side chain of Ile-52 in the tyrosine complex of TyrTS(Cys → Gly-35) and to say qualitatively that both the new and the wild-type conformations are populated in this mutant. However, it is not possible to refine the occupancies and obtain quantitative data. The discussion is restricted, therefore, to the qualitative aspects that seem beyond doubt.

TyrTS(Cys → Gly-35) Mutant

Interpretation of Structural Changes. Two changes in structure in the enzyme–tyrosine complex were observed on mutation of Cys → Gly-35. The side chain of Thr-51 rotates about the C_α–C_β bond so that the γ-methyl group partly occupies the space vacated by the –CH_2-SH of Cys-35. The side chain of Ile-52 becomes disordered. Although glycine residues are the most flexible links in the protein main chain, mutation of Cys → Gly-35, leaves the α-carbon backbone unchanged. The observed changes in structure are thus a consequence of the creation of a cavity in the protein on deletion of the side chain and the movement of side chains of other amino acids to occupy the cavity. In the enzyme–tyrosyl adenylate com-

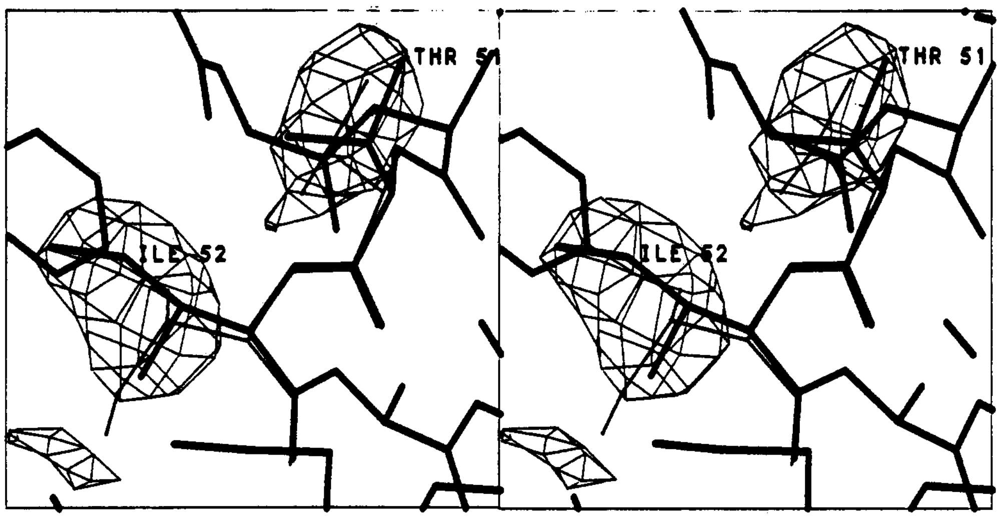

FIGURE 6: Difference electron density map (F_o–F_c, α_{calc}) at 2.7-Å resolution of the Cys → Gly-35 mutant complexed with tyrosyl adenylate, where Thr-51 and Ile-52 side chains have been removed from the model. Contouring is at 3σ, positive density shown only. This figure shows that Thr-51 becomes disordered on formation of enzyme-bound tyrosyl adenylate and the side chain of Ile-52 prefers to adopt the conformation resembling that of the native enzyme (native and mutant in heavy and thin line; respectively).

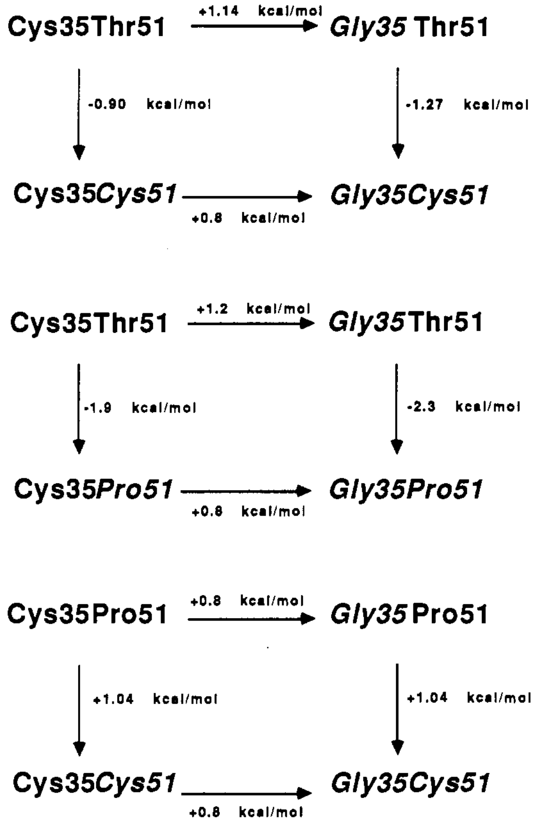

FIGURE 7: Double-mutant data for Cys → Gly-35 paired with Thr → Pro-51 and Thr → Cys-51, respectively (Carter et al., 1983; Fersht et al., 1985). They show a consistent nonadditivity of about 0.4 kcal/mol on going from cysteine to glycine at position 35 when residue 51 is mutated from threonine to either cysteine or proline. The fact that there is no effect on the energetics of the Cys → Gly-35 mutation with either cysteine or proline at residue 51 (final cycle) suggests that there may be an interaction between Thr-51 and Gly-35 in the Cys → Gly-35 mutant. (The small discrepancies in the mutation of Cys → Gly-35 etc. in wild-type enzyme result from the statistical variation in experiments repeated at different times.)

plex, the side chain of Ile-52 tends to revert to the wild-type conformation and Thr-51 becomes disordered.

Relationship between Changes in Structure and Activity and Double-Mutant Tests. Mutation of Cys → Gly-35 in wild-type enzyme weakens the binding of the transition state for the formation of Tyr-AMP by 1.2 kcal/mol (Carter et al., 1984). Mutation of Cys → Gly-35 in either of the mutants, TyrTS(Thr → Pro-51) or TyrTS(Thr → Cys-51), weakens binding by only 0.8 kcal/mol (Fersht et al., 1985a). Expressed as the double-mutant test (Figure 7), the mutations of Cys-35 and Thr-51 are seen to be nonadditive, indicating that the mutations are not independent. Starting from either Pro-51 or Cys-51, however, mutations appear to be independent.[2] The double-mutant data may be interpreted as follows. Starting from wild-type enzyme, mutating Cys → Gly-35 causes changes in the position of the γ-methyl group of Thr-51. Thus, mutations of Thr-51 and Cys-35 are not independent. However, once Thr-51 has been mutated to either Pro or Cys there is no longer the problematic γ-methyl group in the starting state and so there is the possibility of additivity. [Note, the crystal structure of TyrTS(Thr → Cys-51) has been solved (M.D.F., unpublished results) and the γ-SH of Cys-51 does not occupy the same position as the γ-methyl of Thr-51 in the wild-type structure.]

Thermodynamic Data. The X-ray data suggest that the binding of substrate perturbs the equilibrium between two conformations of Ile-52. In the ground state, E·Tyr, Ile-52 has two conformations that are roughly equally populated. In the transition state, Ile-52 occupies primarily just one conformation. There is a loss in entropy of $R \ln 2$ for Ile-52 on formation of the transition state. However, there are unknown energy changes for Thr-51 on going from the E·Tyr to the E·Tyr-AMP complex: Thr-51 presumably increases its enthalpy and entropy as it moves from its ordered state in the TyrTS(Cys → Gly-35)·Tyr complex to its disordered state in the TyrTS(Cys → Gly-35)·Tyr-AMP complex. There is thus a reorganization energy term (Fersht, 1988) on mutation of Cys → Gly-35, and so it is not surprising that there are significant changes in $\Delta H^{\ddagger}$ and $\Delta S^{\ddagger}$ (Wells et al., 1991).

Hydrogen-Bond Inventory of Wild-Type and Mutant Enzymes. The latest crystallographic data suggest that there is not a hydrogen bond between the –SH of Cys-34 and the 3′-OH of the ribose but that the interaction is mediated by a water molecule (water-326, Brick et al., 1989). How does this affect the interpretation of the energetic changes on

---

[2] The energy changes are calculated for the process E·Tyr + ATP → [E·Tyr-ATP]‡ and so the two structures required for quantitative calculation of the energetics should, therefore, be of those two complexes. Fortunately, data from linear free energy relationships and difference energy diagrams indicate that the interactions between the ribose ring and the enzyme are very close in energy to those in the E·Tyr-AMP complex (Fersht et al., 1987).

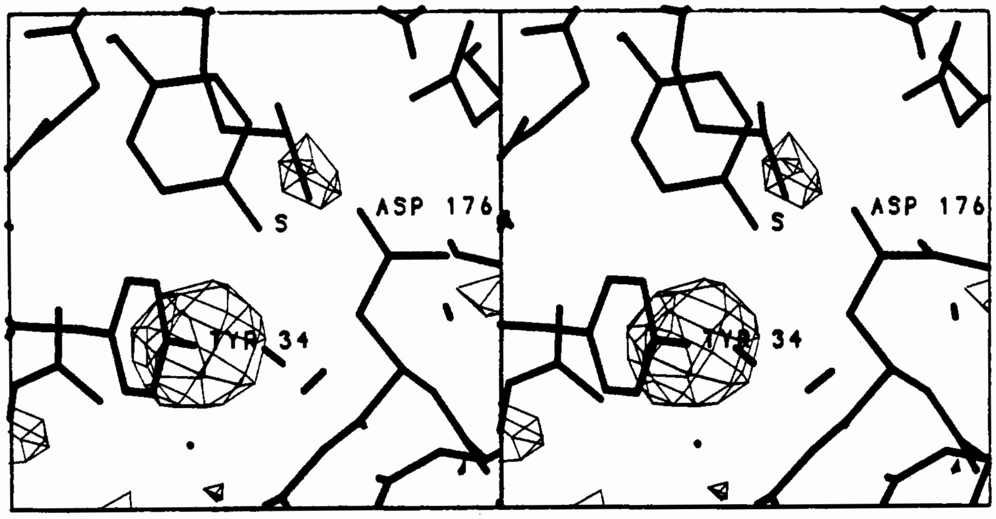

FIGURE 8: Difference electron density map ($F_{mut}-F_{wt}$, α_{wt}) of the mutant Tyr → Phe-34 complexed with tyrosine, at 2.7-Å resolution, contouring at 3σ. Negative density is shown only. The negative peak over the side chain of Tyr-34 in the native model shows the lack of electron density for the hydroxyl group in the mutant structure. The model is that of the native enzyme complexed with tyrosine. The substrate is labeled S.

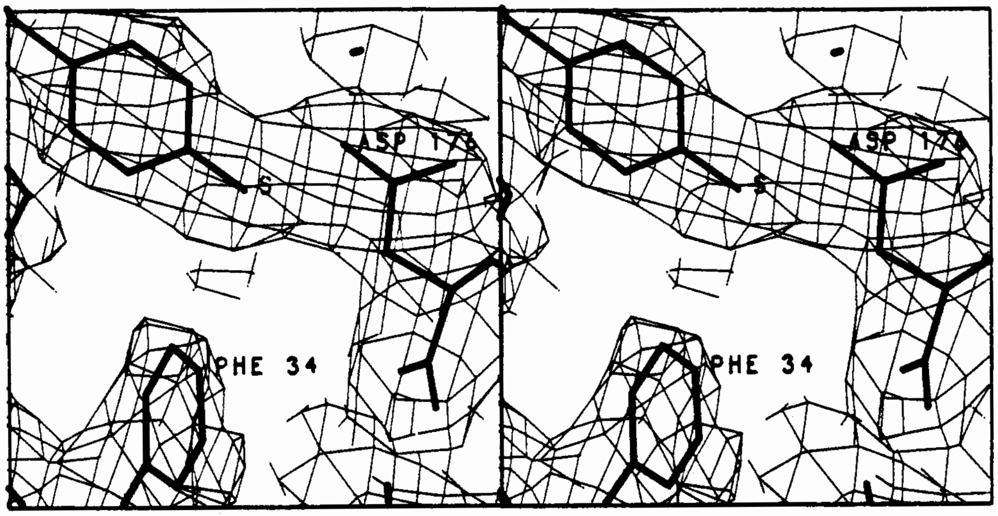

FIGURE 9: Electron density map ($3F_o-2F_c$, α_{calc}) after several cycles of refinement of the Tyr → Phe-34 mutant complexed with tyrosine. The refined native and mutant models are almost identical. Note the clear density for the substrate S. Contouring is at 1σ.

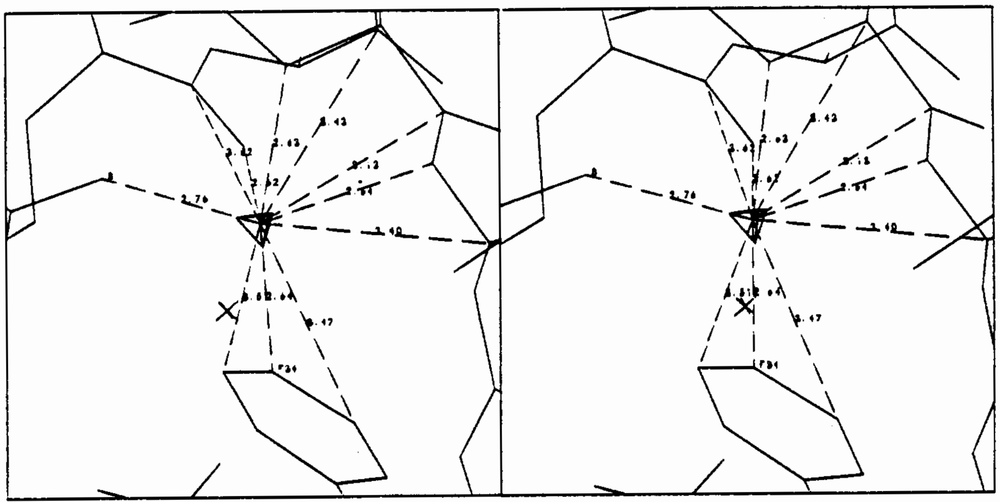

FIGURE 10: A hypothetical water molecule modeled between the substrate hydroxyl and the mutant residue, phenylalanine-34, in the refined structure of the Tyr → Phe-34 mutant. Neighboring residues are too close-packed for this to occur in reality.

mutation? A crude way of examining the effects of changes in hydrogen bonding is to perform a hydrogen-bond inventory, i.e., count the number of hydrogen bonds on each side of the chemical equation since the most important individual energy terms when considering hydrogen bonds is the hydrogen-bond dissociation energy (Fersht et al., 1985b). Direct hydrogen bonding between a substrate (B-S) and an enzyme (E-H) (eq 1) is an exchange reaction whereby two molecules of hydro-

$$\text{E-H}\cdots\text{OH}_2 + \text{OH}_2\cdots\text{B-S} \rightleftharpoons \text{E-H}\cdots\text{B-S} + \text{H}_2\text{O}\cdots\text{H}_2\text{O} \quad (1)$$

gen-bonded water are released. There is just an exchange of hydrogen bonds. Although the hydrogen bond inventory is zero, bonding in the enzyme–substrate complex is favored entropically by the release of water. Because hydrogen bonding is an exchange process, differences in hydrogen-bond strengths tend to cancel. There is not the loss of the full hydrogen-bond dissociation energy on deletion of the hydrogen-bond donor from E-H even when there is an unpaired acceptor in the E·S complex (eq 2) since, in effect, the hydrogen-bond inventory is still zero (Fersht et al., 1985b; Fersht, 1987b).

$$\text{E/OH}_2 + \text{OH}_2\cdots\text{B-S} \rightleftharpoons \text{E/B-S} + \text{H}_2\text{O}\cdots\text{H}_2\text{O} \quad (2)$$

In some cases, there will be room for solvent water to have access to the substrate when bound and form a bond with B (eq 3). In this situation, ΔG_{app} approximates to the true incremental binding energy (Fersht, 1987a, 1988).

$$\text{E/OH}_2 + \text{OH}_2\cdots\text{B-S} \rightleftharpoons \text{E/OH}_2\cdots\text{B-S} + \text{H}_2\text{O} \quad (3)$$

In an example as here with Cys-35, where a water molecule bridges the donor and acceptor on the enzyme and substrate, only one water molecule is displaced (eq 4). This is less favorable entropically than in eq 1 because only one water molecule is released.

$$\text{E-H}\cdots\text{OH}_2 + \text{H}_2\text{O}\cdots\text{B-S} \rightleftharpoons \text{E-H}\cdots\text{H}_2\text{O}\cdots\text{B-S} + \text{H}_2\text{O} \quad (4)$$

On deletion of the hydrogen-bond donor on the enzyme (eq 5), the hydrogen bond inventory does not formally change. The precise energetics depend of course on the precise interactions. The inventory simply illustrates the changes in hydrogen-bonding interactions.

$$\text{E/OH}_2 + \text{H}_2\text{O}\cdots\text{B-S} \rightleftharpoons \text{E/H}_2\text{O}\cdots\text{B-S} + \text{H}_2\text{O} \quad (5)$$

The observations from the structural study and from the double-mutant test (Figure 7) show that the mutation Cys → Gly-35 in wild-type enzyme has complications in addition to those on removal of the (indirect) hydrogen bond between the -SH of Cys-35 and the 3′-OH of the substrate. The apparent H-bond strength at position 35 is better measured from mutation of Cys → Gly-35 is either TyrTS(Thr → Pro-51) or TyrTS(Thr → Cys-51) where the free energy changes are additive. The value of ΔG_{app} is 0.8 kcal/mol in both cases for the binding energy in the transition state. It is evident from the crystal structure of TyrTS(Cys → Gly-35)·Tyr-AMP complex that there is access of water to the 3′-OH of Tyr-AMP.

The value of ΔG_{app} for the mutation Cys → Gly-35 in wild-type enzyme increases as the reaction proceeds, being negligible in the E·Tyr·ATP complex, 1.2 kcal/mol in the transition state, and 1.6 kcal/mol in the E·Tyr-AMP complex (Wells & Fersht, 1985, 1986). This was considered interesting as it showed that there is a better complementarity of the enzyme towards the enzyme-bound intermediate than to the transition state in this region. This was rationalized on the basis of it being necessary for the Tyr-AMP to be bound tightly. The demonstration here that there is a significant ΔG_{reorg} component to ΔG_{app} does not invalidate the previous arguments. First, as pointed out by Fersht (1988), the important quantity for interpretation is not ΔG_{app} but $\Delta\Delta G_{\text{app}}$, the change in ΔG_{app} from one step to the next on the reaction pathway, as this can be equal to the true change in binding energy as the reaction proceeds—this holds when $\Delta\Delta G_{\text{reorg}}$ is zero. Second, experiments on the mutant TyrTS(Cys → Ser-35), which still retains a significantly sized side chain, give values of $\Delta\Delta G_{\text{app}}$ data that are very similar to those for TyrTS(Cys → Gly-35) [$\Delta G_{\text{app}} = 1.2$ kcal/mol for binding the transition state and $\Delta G_{\text{app}} = 1.5$ kcal/mol for binding Tyr-AMP (Wells & Fersht, 1986)].

Binding of Tyrosine to ΔTyrTS(Tyr → Phe-34). There are no observed structural changes in the E·Tyr complex on mutating Tyr → Phe-34 apart from the replacement by an –H of the –OH group. There is also no room for a water molecule to occupy the space in ΔTyrTS(Tyr → Phe-34) formerly occupied by that –OH group. The –OH of bound Tyr-AMP is thus not paired with a hydrogen-bond donor. The measured value of ΔG_{app} on mutation of Tyr → Phe-34 does not measure the incremental binding energy of the hydrogen bond but must be described by equations given by Fersht (1988). The observed value of ΔG_{app} of 0.5 kcal/mol is low. This is in accord with a simple hydrogen-bond inventory.

Conclusions. Kinetic tests had indicated that mutation of Cys → Gly-35 in TyrTS could involve minor structural changes and these have now been observed. Conversely, kinetics and logic suggested that mutation of Tyr → Phe-34 should cause little effect other than removal of the oxygen atom. Direct structural observation reveals that there are no changes at the level of resolution of the crystal structures. The crystal structures have aided the interpretation of apparent binding energy changes on mutation.

ACKNOWLEDGMENTS

We gratefully acknowledge the hospitality, help, and patient tuition from David Blow, Peter Brick, and Kim Henrick at Imperial College of Science, Technology and Medicine.

Registry No. Cys, 52-90-4; Tyr, 60-18-4; tyrosyl-tRNA synthetase, 9023-45-4; tyrosyl adenylate, 50466-77-8.

REFERENCES

Barker, D. G., & Winter, G. (1982) *FEBS Lett. 145*, 191–193.

Blow, D. M., & Brick, P. (1985) in *Biological Macromolecules and Assemblies: Nucleic Acids and Interactive Proteins* (Jurnak, F., & McPherson, A., Eds.) Vol. 2, pp 442–469, Wiley, New York.

Brick, P., & Blow, D. M. (1987) *J. Mol. Biol. 194*, 287–297.

Brick, P., Bhat, T. N., & Blow, D. M. (1989) *J. Mol. Biol. 208*, 83–98.

Carter, P. J., Winter G., Wilkinson A. J., & Fersht, A. R. (1984) *Cell (Cambridge, Mass.) 38*, 835–840.

Fersht, A. R. (1987a) *Biochemistry 26*, 8031–8037.

Fersht, A. R. (1987b) *Trends Biochem. Sci. 12*, 301–304.

Fersht, A. R. (1988) *Biochemistry 27*, 1577–1580.

Fersht, A. R., Leatherbarrow, R. J., & Wells, T. N. C. (1982) *Nature (London) 322*, 284–286.

Fersht, A. R., Wilkinson, A. J., Carter, P. J., & Winter, G. (1985a) *Biochemistry 24*, 5858–5861.

Fersht, A. R., Shi, J. P., Knill-Jones, J., Lowe, D. M., Wilkinson, A. J., Blow, D. M., Brick, P., Carter, P., Waye, M. M. Y., & Winter, G. (1985b) *Nature (London) 316*, 656–657.

Fersht, A. R., Knill-Jones, J. W., Bedouelle, H., & Greg Winter (1988) *Biochemistry 27*, 1581–1587.

Hendrickson, W. A. (1985) *Methods Enzymol. 115*, 253–270.

Irwin, M. J., Nyborg, J., Reid B. R., & Blow, D. M. (1976) *J. Mol. Biol. 105*, 577–586.

Jones, T. A. (1985) *Methods Enzymol. 115*, 157–171.

Lowe, D. M., Fersht, A. R., Wilkinson A. J., Carter P., & Winter G. (1985) *Biochemistry 24*, 5106–5109.

Lowe, D. M., Winter, G., & Fersht, A. R. (1987) *Biochemistry 26*, 6038–6043.

McPherson, A. (1982) *The Preparation and Analysis of Protein Crystals*, Wiley, New York.

Nyborg, J., & Wonnacott, A. J. (1977) *The Rotation Method* *in Crystallography*, North-Holland, Amsterdam.

Rubin, J., & Blow, D. M., (1981) *J. Mol. Biol. 145*, 489–500.

Ponder, J. W., & Richards, F. M. (1987) *J. Mol. Biol. 193*, 775–791.

Waye, M. M. Y., Winter, G., Wilkinson, A. J., & Fersht, A. R (1983) *EMBO J. 2*, 1827–1829.

Wells, T. N. C., & Fersht, A. R. (1985) *Nature (London) 316*, 656–657.

Wells, T. N. C., & Fersht, A. R. (1986) *Biochemistry 25*, 1881–1886.

Wells, T. N. C., Knill-Jones, J. W., Gray, T. E., & Fersht, A. R. (1991) *Biochemistry* (preceding paper in this issue).

Wilkinson, A. J., Fersht, A. R., Blow, D. M., & Winter, G. (1983) *Biochemistry 22*, 3581–3586.

Winter, G., Fersht, A. R., Wilkinson, A. J.; Zoller, M., & Smith, M. (1982) *Nature (London) 299*, 756–758.

Carboxyl-Terminal Peptides as Probes for *Escherichia coli* Ribonucleotide Reductase Subunit Interaction: Kinetic Analysis of Inhibition Studies[†]

Isabel Climent and Britt-Marie Sjöberg*
Department of Molecular Biology, Stockholm University, S-10691 Stockholm, Sweden
Charles Y. Huang
Laboratory of Biochemistry, National Heart, Lung and Blood Institute, National Institutes of Health, Bethesda, Maryland 20892

Received November 19, 1990; Revised Manuscript Received February 7, 1991

ABSTRACT: The active complex of *Escherichia coli* ribonucleotide reductase comprises two dissociable, nonidentical homodimeric proteins, B1 and B2. When B2 is the varied component, the reductase activity is competitively inhibited by synthetic peptides of varying lengths corresponding to the C-terminus of protein B2. This finding provides the first evidence that the C-terminal peptides and protein B2 share the same binding domain on protein B1. Our data also show that two molecules of peptide can bind to protein B1 with equal affinity. Similar inhibition constants (18 μM) were obtained for peptides containing the C-terminal 20, 30, and 37 residues. When the invariant residue Tyr 356 was omitted, a 2-fold decrease in peptide inhibitory ability was observed. A small peptide, lacking the last 11 residues, had virtually no inhibitory potency. These results, coupled with our previous observations that truncated protein B2, in which one or both polypeptide chains are missing approximately 24 C-terminal residues, had considerably lower or no affinity for B1, suggest that the C-terminal regions are the major determinants in the B1–B2 interaction. In the Appendix, two methods for treatment of kinetic situations pertinent to the ribonucleotide reductase system are presented. One method deals with the determination of kinetic parameters for two components present at comparable levels; the other is concerned with the differentiation of linear and nonlinear competitive inhibition involving the binding of two inhibitor molecules. Both methods should find application to other similar cases.

Ribonucleotide reductase is an essential enzyme for DNA synthesis in all living cells. By reducing ribonucleotides to the corresponding deoxyribonucleotides, the enzyme provides the cells with the precursors needed for DNA synthesis. The *Escherichia coli* enzyme has been extensively studied and has been shown to serve as a prototype for the eukaryotic ribonucleotide reductases. It consists of two nonidentical homodimeric proteins (α_2 and β_2), denoted B1 and B2, respectively [for review, cf. Erikson and Sjöberg (1989)]. Protein B1 contains binding sites for substrates and allosteric regulators and the redox-active cysteines (Reichard, 1988; Åberg et al., 1989; Stubbe, 1989). Protein B2 contributes the tyrosyl radicals and the iron centers (Larsson et al., 1986; Sahlin et al., 1989; Lynch et al., 1989; Nordlund et al., 1990). Proteins B1 and B2 are purified separately, and each is inactive by itself. The active form of the enzyme is the $\alpha_2\beta_2$ complex which can form by a Mg^{2+}-dependent association of B1 and B2.

Little is known about the interaction between subunits in the active complex of ribonucleotide reductase. Evidence from the *E. coli* enzyme suggests that the C-terminal ends of the B2 protein are involved in the interaction with the B1 protein. A heterodimeric form of protein B2, which contains one full-length and one truncated polypeptide chain lacking approximately 24 C-terminal residues,[1] binds poorly to protein B1; the truncated homodimeric form does not bind at all (Sjöberg et al., 1987). Experiments with the enzyme from herpes simplex virus have shown that a nonapeptide representing the C-terminal region of the H2 protein (the viral B2 counterpart) inhibited the viral enzyme activity, but had no effect on the cellular enzyme (Cohen et al., 1986; Gaudreau et al., 1987). This finding indicates that the nonapeptide interferes with the association between H1 and H2. In two recent studies Yang et al. (1990) and Consentino et al. (1990) reported efficient crossinhibition of calf thymus enzyme by

---

[†] The research was supported in part by grants from the Swedish Cancer Society and Wenner-Grenska Samfundet.

[*] To whom correspondence should be addressed.

[1] The number of missing residues in the truncated protein B2 was thought to be 30; it has been redetermined to be 24 (or 22) (M. Karlsson, unpublished results).

0006-2960/91/0430-5164$02.50/0